

# Broad-band and high-temperature ultrasonic transducer fabricated using a $\text{Pb}(\text{In}_{1/2}\text{Nb}_{1/2})\text{-Pb}(\text{Mg}_{1/3}\text{Nb}_{2/3})\text{-PbTiO}_3$ single crystal/epoxy 1–3 composite

Dan Zhou,<sup>1</sup> Kwok Fung Cheung,<sup>1</sup> Kwok Ho Lam,<sup>1</sup> Yan Chen,<sup>1</sup> Yat Ching Chiu,<sup>1</sup> Jiyan Dai,<sup>1,a)</sup> Helen Lai Wa Chan,<sup>1</sup> and Haosu Luo<sup>2</sup>

<sup>1</sup>Department of Applied Physics and Materials Research Centre, The Hong Kong Polytechnic University, Hong Kong, China

<sup>2</sup>Information Materials and Devices Research Center, Shanghai Institute of Ceramics, Chinese Academy of Science, Shanghai 201800, China

(Received 2 March 2011; accepted 31 March 2011; published online 19 May 2011)

In this paper, 1–3 composites based on  $\text{Pb}(\text{In}_{1/2}\text{Nb}_{1/2})\text{-Pb}(\text{Mg}_{1/3}\text{Nb}_{2/3})\text{-PbTiO}_3$  (PIMNT) single crystal and high-temperature epoxy were fabricated with various volume fractions of PIMNT single crystal ranging from 0.4 to 0.9. The electrical properties were studied as functions of PIMNT volume fraction and temperature, and it revealed that the nature of ultrahigh electromechanical coupling coefficient (0.82–0.93) and low acoustic impedance (17–19 MRayl) of the composites can be retained within a wide temperature range from room temperature to 185 °C. Single element ultrasonic transducer using the PIMNT 1–3 composite was fabricated and characterized as a function of temperature. It was found that the transducer can still work normally at high temperatures, such as 165 °C, possessing a bandwidth of 95% and insertion loss of –27 dB. © 2011 American Institute of Physics. [doi:10.1063/1.3583746]

## I. INTRODUCTION

Relaxor-based ferroelectric single crystals  $\text{Pb}(\text{Mg}_{1/3}\text{Nb}_{2/3})\text{-PbTiO}_3$  (PMNT) and  $\text{Pb}(\text{Zn}_{1/3}\text{Nb}_{2/3})\text{-PbTiO}_3$  have attracted considerable attention because of their ultrahigh electromechanical coupling factors and piezoelectric coefficients near the morphotropic phase boundary composition.<sup>1–4</sup> Based on their excellent performance, various applications such as those in ultrasonic motors, transducers, and actuators,<sup>5–8</sup> have been proposed. However, these binary single crystals have low Curie temperatures ( $T_c$ ) of about 130–170 °C at which depolarization occurs easily in high-temperature applications.<sup>3,9</sup> Besides, even though the working temperature is lower than  $T_c$ , the electrical properties may start to degrade during the transition from rhombohedral to tetragonal phases at specific temperatures ( $T_{\text{IT}}$ ) of around 60–95 °C.<sup>10–12</sup> In order to overcome the limitation, a ternary single crystal  $\text{Pb}(\text{In}_{1/2}\text{Nb}_{1/2})\text{-Pb}(\text{Mg}_{1/3}\text{Nb}_{2/3})\text{-PbTiO}_3$  (PIMNT) with a high  $T_c$  of 200 °C was grown from the melt directly by the Bridgman method. Its excellent piezoelectric properties were reported to be maintained within a boarder temperature range.<sup>13–16</sup> This allows greater flexibility of device design especially for high-power and high-temperature applications.

Using a 1–3 connectivity, the behavior of the PIMNT single crystal can be further improved for ultrasonic transducer applications. First, the structure of the 1–3 composite reduces the lateral vibration mode and utilizes a high longitudinal coupling coefficient  $k_{33}$  (90%) instead of a low thickness coupling coefficient  $k_t$  (59%), leading to much efficient conversion between electrical and mechanical energy as compared with the single phase material. Second, the structure of the 1–3 composite would lower the acoustic impedance  $Z$  and

mechanical quality factor  $Q_m$ , being beneficial in broad-band transducers design. The acoustic impedance of the PIMNT single crystal ( $\sim 37$  MRayl) is much higher than that of the common acoustic loads, such as human tissues ( $\sim 1.5$  MRayl) for biomedical ultrasound applications and ultrasonic coupler ( $< 2.5$  MRayl) for industrial non-destructive detections. This acoustic impedance mismatch causes a long ring-down echo due to the reflection at the interface between a vibrator and an acoustic load. Third, the dielectric property of the 1–3 composite can be easily tuned by varying the active phase volume fraction. As a consequence, the electrical properties of the transducer using this kind of composites can be easily adjusted to match the driving and receiving electronics.

In this work, the PIMNT single crystal/epoxy 1–3 composites, i.e., PIMNT columns in a passive epoxy matrix, were prepared and systematically investigated as a function of PIMNT single crystal volume fraction. The temperature stability of the dielectric, piezoelectric, and acoustic properties was also investigated. In addition, a single-element ultrasonic transducer was designed and fabricated according to the performance of the prepared PIMNT/epoxy 1–3 composite. It was found that the transducer can maintain reasonably good performance at temperatures approaching the high Curie temperature of PIMNT single crystal.

## II. FABRICATION AND CHARACTERIZATION OF PIMNT/EPOXY 1–3 COMPOSITES

PIMNT single crystal with the nominal composition of  $0.24\text{Pb}(\text{In}_{1/2}\text{Nb}_{1/2})\text{-}0.45\text{Pb}(\text{Mg}_{1/3}\text{Nb}_{2/3})\text{-}0.31\text{PbTiO}_3$  (PIMNT 24/45/31) was grown by a modified Bridgman method. The as-grown [001] oriented single crystal was diced into square plates with dimensions of 15 mm  $\times$  15 mm  $\times$  2 mm. The 1–3 composites with different PIMNT volume fractions ( $\phi$ )

<sup>a)</sup>Fax: +852-2333-7629. Electronic mail: apdaijy@inet.polyu.edu.hk

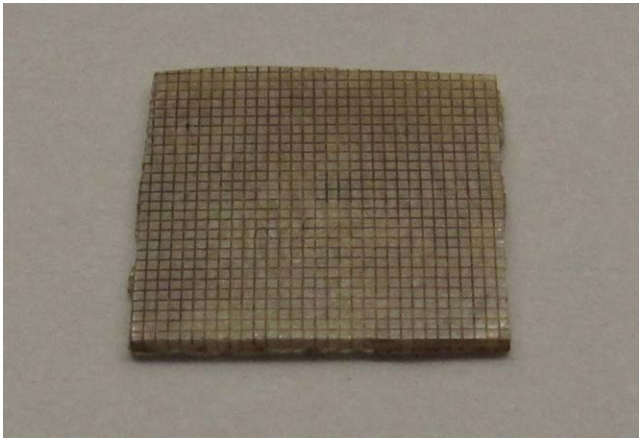


FIG. 1. (Color online) Photograph of the fabricated PIMNT single crystal/epoxy 1–3 composites.

were fabricated using the dice and fill method.<sup>17</sup> A 50  $\mu\text{m}$ -thick blade of a dicing saw (DAD 321, DISCO, Japan) was used to dice the crystal, and a low dicing speed of 0.46 mm/s was adopted to avoid breaking the fragile PIMNT single crystal in the process. Araldite GY251/Aradur HY956 (100:20) epoxy was used to fill the kerfs, due to its higher working temperature ( $<300^\circ\text{C}$ ) as compared with the common epoxy ( $<100^\circ\text{C}$ ). The epoxy matrix was evacuated before solidification in order to remove the trapped bubbles. After curing the epoxy, the top and bottom sides of the composites were ground to remove the bulk PIMNT single crystal support layer and the excess epoxy, respectively (Fig. 1). After depositing a 500-nm-thick chromium/gold (Cr/Au) electrode on both sides of the 1–3 composites by magnetron sputtering, the composites were poled at room temperature under a dc electric field of 2.5 kV/mm for 15 min.

The performance of the 1–3 composites was simulated by the modified series and parallel model.<sup>18,19</sup> Since the lateral spatial scale of the fabricated composites is sufficiently fine, the composites can be treated as an effective homogeneous medium. The elastic, dielectric, piezoelectric, electromechanical, and acoustic parameters, which are very useful for transducer design, were modeled in terms of the volume fraction of PIMNT single crystal, as shown in Fig. 2 (lines).

The piezoelectric  $d_{33}$  coefficient of the 1–3 composites was measured along the thickness direction by a  $d_{33}$  meter (ZJ-3A, Beijing Institute of Acoustics, Chinese Academy of Sciences). According to the IEEE Standards on Piezoelectricity,<sup>20</sup> the thickness electromechanical coupling coefficient  $k_t$  is expressed by the following relation:

$$k_t = \sqrt{\frac{\pi}{2} \frac{f_r}{f_a} \tan\left(\frac{\pi}{2} \frac{f_a - f_r}{f_a}\right)}, \quad (1)$$

where  $f_r$  and  $f_a$  are the resonant and anti-resonant frequencies, respectively, which were obtained using an impedance analyzer (Agilent 4294A, USA). The clamped dielectric constant  $\epsilon_{33}^S$  was determined by measuring the capacitance  $C$  at a high

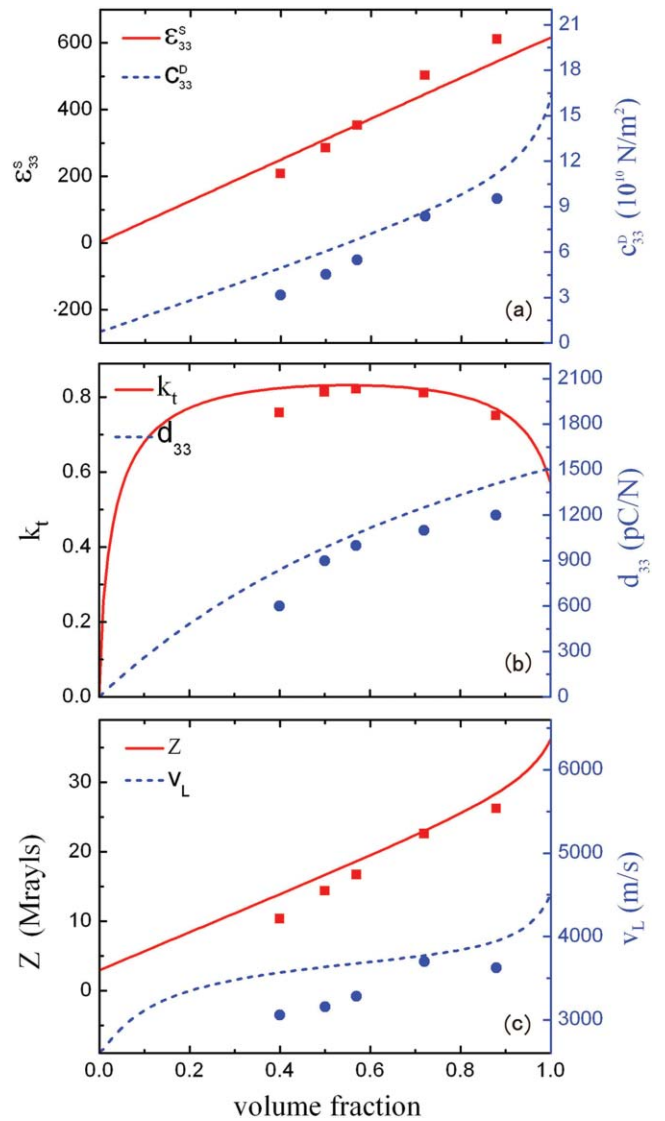


FIG. 2. (Color online) Comparison between simulation results (lines) and measured results (points) of the properties of the PIMNT single crystal/epoxy 1–3 piezocomposites as a function of  $\phi$ : (a) dielectric constant ( $\epsilon_{33}^S$ ) and elastic stiffness ( $c_{33}^D$ ); (b) thickness electromechanical coupling coefficient ( $k_t$ ) and piezoelectric constant ( $d_{33}$ ); (c) acoustic velocity ( $v_L$ ) and acoustic impedance ( $Z$ ).

frequency of 10 MHz:

$$\epsilon_{33}^S = \frac{Ct}{S\epsilon_0}, \quad (2)$$

where  $S$  and  $t$  are the electroded area and thickness of the 1–3 composites, respectively, and  $\epsilon_0$  is the permittivity of free space. The stiffness constant  $c_{33}^D$  under constant electric displacement  $D$  was determined from the impedance spectrum

$$c_{33}^D = \rho (2tf_a)^2, \quad (3)$$

where the density  $\rho$  of the composite was measured according to Archimedes' principle. The sound velocity  $v_L$  and acoustic impedance  $Z$  were calculated from the following formulas:

$$v_L = 2tf_a, \quad (4)$$

$$Z = \rho v_L. \quad (5)$$

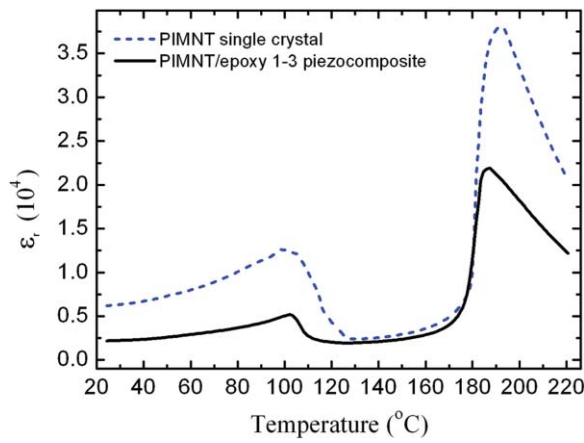


FIG. 3. (Color online) Temperature dependence of the dielectric constant ( $\epsilon_r$ ) of the [001]-poled rhombohedral PIMNT single crystal and its 1-3 piezocomposite with  $\phi = 0.72$ .

Figure 2 shows the modeled (lines) and measured (dots) properties of the PIMNT single crystal/epoxy 1-3 composites with different volume fractions of PIMNT single crystal. It is shown that  $\epsilon_{33}^S$ ,  $c_{33}^D$ ,  $d_{33}$ ,  $v_L$ , and  $Z$  increase with the PIMNT volume fraction. The  $k_t$  value of the composites can reach as high as 82%, which is much higher than that of the [001]-oriented PIMNT single crystal (59%). Besides, the  $d_{33}$  value of the composite can approach 1000 pC/N when  $\phi$  is 0.57. From the obtained results, the properties of the PIMNT single crystal/epoxy 1-3 composites basically agree with the prediction, and are obviously superior to those of commercial PZT ceramics and their 1-3 composites. The results show that the 1-3 composites have several advantages compared with the single phase material, such as high electromechanical coupling coefficient, low acoustic impedance, and moderate dielectric constant. Table I summarizes the material properties of the PIMNT single crystal and its 1-3 composites with different PIMNT volume fractions. Other common piezoelectric materials are also involved for comparison.

Figure 3 shows the temperature-dependent dielectric properties of the PIMNT single crystal and its 1-3 composite with  $\phi = 0.72$ . The dielectric constant  $\epsilon_r$  was measured at 1 kHz by means of a computer-controlled impedance analyzer with the temperature ranging from 25 to 220 °C. It can be seen that there are two dielectric peaks around 105 °C and 195 °C, which are the transition temperatures from ferroelectric rhombohedral phase to ferroelectric tetragonal phase ( $T_{rt}$ ) and from ferroelectric tetragonal phase to paraelectric cubic phase ( $T_c$ ), respectively.

Figure 4 shows the temperature-dependent  $f_r$  and  $f_a$ , calculated  $k_t$ ,  $v_L$ , and  $Z$  of the PIMNT single crystal/epoxy 1-3 composites with  $\phi$ . Below  $T_{rt}$ , both  $f_r$  and  $f_a$  decrease as the temperature increases. Since the decrement of  $f_r$  is faster than that of  $f_a$ , according to Eq. (1), the corresponding  $k_t$  increases with temperature. When the temperature closes to  $T_{rt}$ ,  $f_r$  starts to increase and then reaches a regional maximum beyond  $T_{rt}$ . As  $f_a$  has no obvious variation, the resultant  $k_t$  changes inversely with  $f_r$ . When the temperature reaches  $T_c$ ,  $f_a$  has a large decrease suddenly so that the  $k_t$  also drops sharply near  $T_c$ .

TABLE I. Material properties of PIMNT single crystal and its 1-3 composites with different PIMNT volume fractions measured at room temperature in comparison with other common piezoelectric materials.

Property	PZT-5H ceramic (Refs. 21 and 22)	PZT/epoxy 1-3 composite (Ref. 23)	PMNT single crystal (Ref. 12)	PMNT/epoxy 1-3 composite (Refs. 24 and 25)	PIMNT single crystal	PIMNT/epoxy 1-3 composite
Dielectric constant $\epsilon_{33}^T$ ( $\epsilon_0$ )	3100	400-1000	5400	300-1800	5370	700-2200
Piezoelectric constant $d_{33}$ (pC/N)	600	300-400	1540	800-1400	1500	600-1200
Coupling coefficient $k_{33}$	0.71		0.91		0.90	
Coupling coefficient $k_t$	0.51	0.58-0.63	0.60	0.75-0.80	0.59	0.75-0.82
Longitudinal velocity $c$ (m/s)	3900		4600	3400-4000	4550	3000-3700
Acoustic impedance $Z_t$ (MRayl)	34	8-20	37	15-20	36.5	10-26

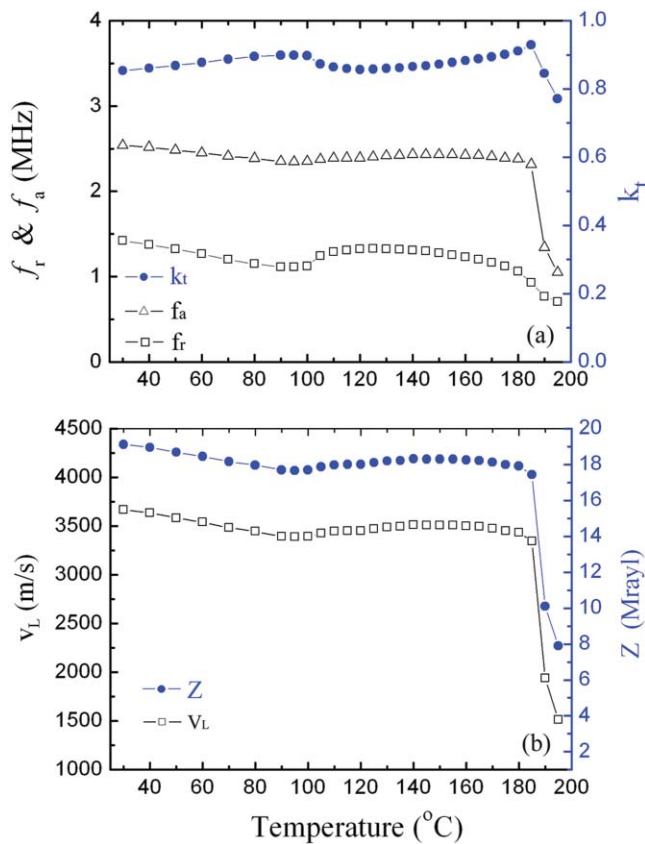


FIG. 4. (Color online) (a) Temperature dependence of the resonant ( $f_r$ ) and anti-resonant frequency ( $f_a$ ) and the calculated thickness electromechanical coupling coefficient ( $k_t$ ); (b) the acoustic velocity ( $v_L$ ) and acoustic impedance ( $Z$ ) of the PIMNT single crystal/epoxy 1-3 piezocomposite with  $\phi = 0.57$ .

When the temperature increases beyond  $T_c$ , the 1-3 composites are considered to be depolarized gradually. As observed from Fig. 4,  $k_t$  retains a reasonably high value ( $>82\%$ ) from room temperature to 190  $^{\circ}\text{C}$ . The maximum  $k_t$  value of 93% is found at 185  $^{\circ}\text{C}$ . For the values of  $v_L$  and  $Z$ , the variation is small with the similar trend of  $f_a$ . From room temperature to 185  $^{\circ}\text{C}$ , the average value of  $v_L$  and  $Z$  is 3500 m/s and 18 MRayl, respectively.

### III. TRANSDUCER DESIGN, FABRICATION, AND RESULTS

In order to acquire high sensitivity and broad bandwidth in transducer applications, the transducer element should have good piezoelectric and electromechanical performance, and relatively low acoustic impedance. As shown in Fig. 2, the composite with  $\phi = 0.5$  shows the optimum performance for the applications of ultrasonic transducer as follows:  $\epsilon_{mn}^T = 285 \epsilon_0$ ,  $d_{33} = 900 \text{ pC/N}$ ,  $k_t = 82\%$ , and  $Z = 15 \text{ MRayl}$ . Thus, the as-prepared PIMNT/epoxy 1-3 composite with  $\phi = 0.5$  was chosen to fabricate a single-element ultrasonic transducer. The thickness of the 1-3 composite was prepared to be 0.5 mm, and the surface area was cut to be 7.5 mm diameter.

The schematic diagram of the designated single-element ultrasonic transducer is shown in Fig. 5. For high tempera-

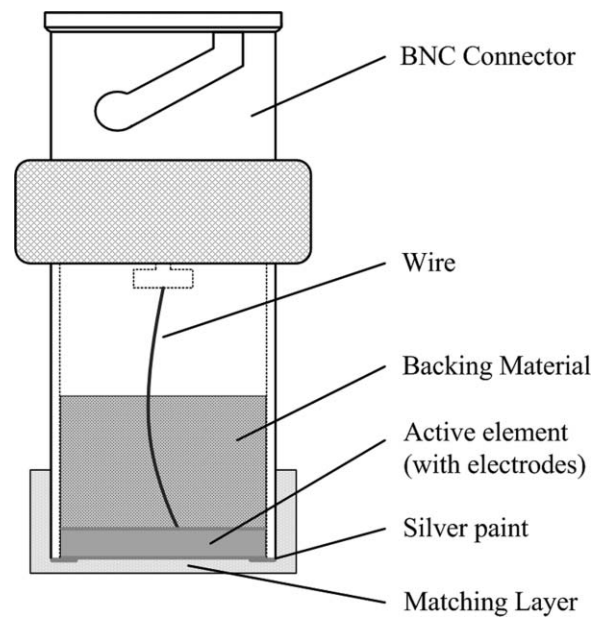


FIG. 5. Schematic diagram of the PIMNT/epoxy 1-3 composite single-element ultrasonic transducer.

ture applications, all the components of the transducer should be able to endure high temperature at which the temperature is higher than the Curie point of the PIMNT single crystal. The front electrode of the PIMNT/epoxy 1-3 composite was connected to the stainless steel housing using an air-drying silver paint (Agar Scientific Ltd., Stansted, Essex CM24 8DA UK), and the back electrode was welded to a core wire of the coaxial cable. The backing material was made by mixing Araldite GY251/Aradur HY956 epoxy and coarse alumina particles (200  $\mu\text{m}$  in diameter). The acoustic waves reflected backwards could be scattered and absorbed by the alumina particles in order to reduce the ring-down time of the transducer. A front-face matching layer with a thickness of  $\lambda/4$  was employed, where  $\lambda$  is the wavelength of the acoustic wave emitted by the 1-3 composite at its resonant frequency. The designated acoustic impedance of the single matching layer



FIG. 6. (Color online) Photograph of the fabricated PIMNT/epoxy 1-3 composite single-element ultrasonic transducer.

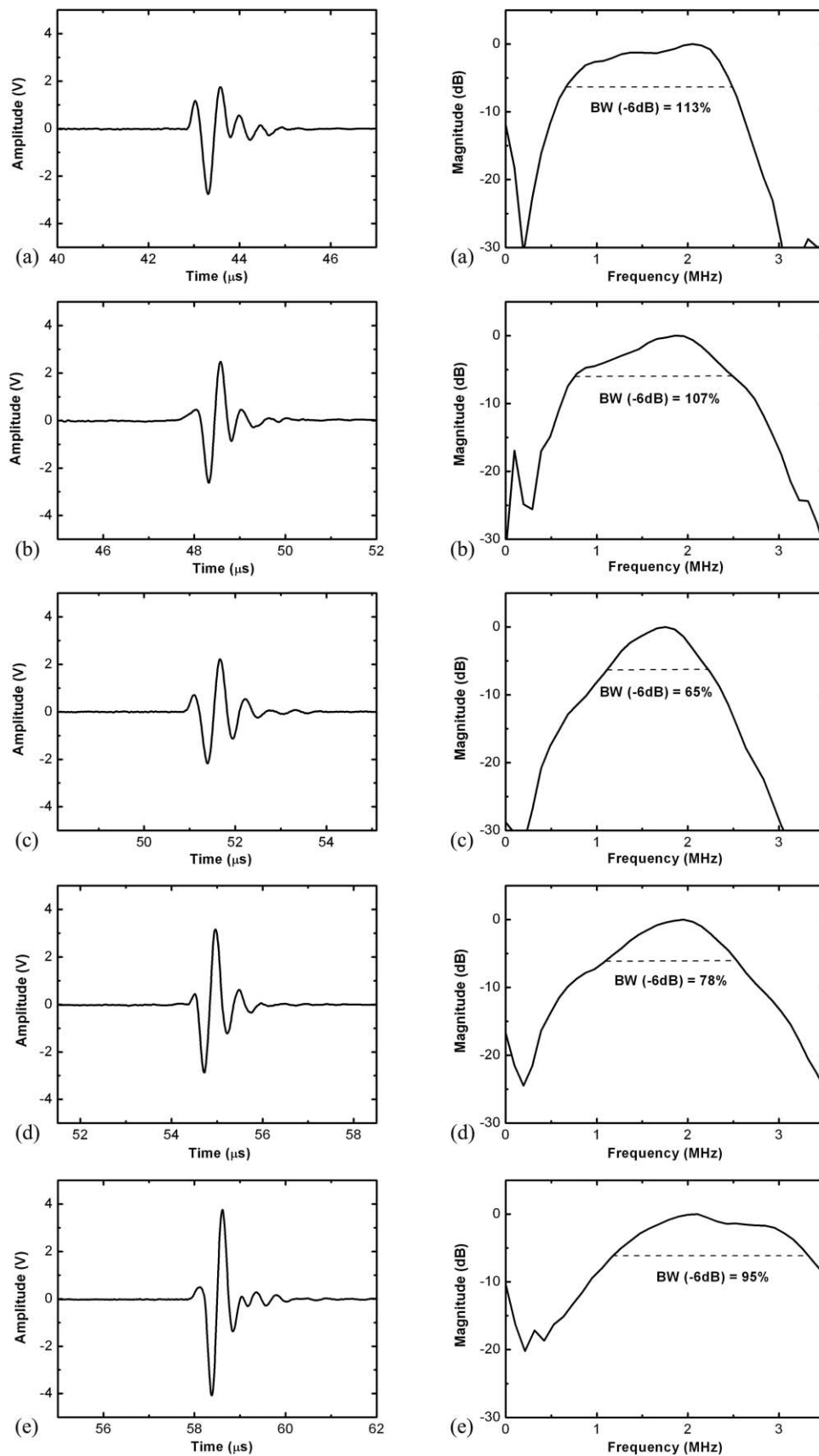


FIG. 7. Pulse-echo waveform and frequency spectra of the PIMNT/epoxy 1-3 composite single-element ultrasonic transducer measured at several temperatures: (a) 45 °C, (b) 80 °C, (c) 105 °C, (d) 125 °C, and (e) 165 °C.

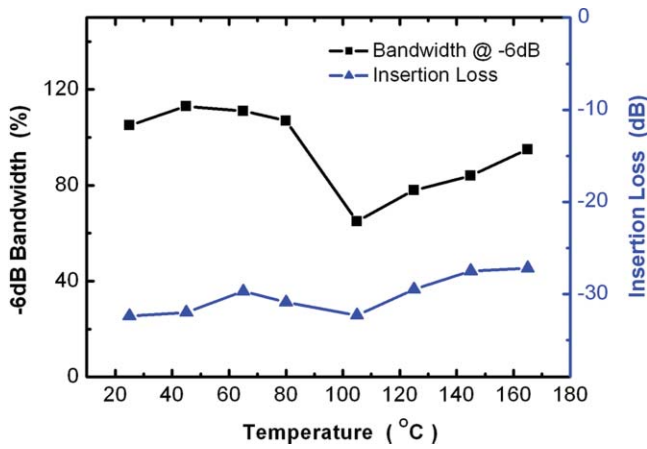


FIG. 8. (Color online) Temperature dependence of the bandwidth and insertion loss of the PIMNT/epoxy 1–3 composite single-element ultrasonic transducer.

( $Z_1 = 3.2 \text{ MRayl}$ ) was calculated as follows:<sup>26</sup>

$$Z_1 = Z_0^1/3Z_L^{2/3}, \quad (6)$$

where  $Z_0$  (15 MRayl) is the acoustic impedance of the PIMNT/epoxy 1–3 composite with  $\phi = 0.5$ , and  $Z_L$  ( $\sim 1.5 \text{ MRayl}$ ) is the acoustic impedance of the load medium (i.e., body tissue and water). In this work, the matching layer was made by mixing Araldite GY251/Aradur HY956 epoxy and fine alumina particles of  $\sim 5 \mu\text{m}$  in diameter. Both the matching layer and backing layer were cured at room temperature for 3 h and then heated to 160 °C with a heating rate of 20 °C/h. Figure 6 shows a photograph of the fabricated single-element ultrasonic transducer. The transducer can be connected to a high-temperature coaxial cable by a BNC connector for subsequent measurements. For measuring the pulse-echo response and insertion loss, the transducer was mounted on a holder and immersed in a silicone oil tank in front of a stainless steel block. The transducer was placed such that the reflector was at the near field/far field transition point  $T$ , approximately given by

$$T = \frac{a^2}{\lambda}, \quad (7)$$

where  $a$  is the radius of the transducer element ( $= 3.75 \text{ mm}$ ) and  $\lambda$  is the wavelength in silicone oil at the centre frequency of the transducer. By connecting to an ultrasonic pulser-receiver (Panametrics 5900PR, Olympus, Japan), the transducer was excited by a 1  $\mu\text{J}$  electrical impulse with 1 kHz repetition rate and 50  $\Omega$  damping factor. The echo response was captured and displayed on an oscilloscope (Infinium 54810A, HP/Agilent, USA). The built-in fast Fourier transform (FFT) feature of the oscilloscope was used to compute the frequency spectrum of the pulse-echo response. The  $f_c$  and BW of the transducer were determined from the measured FFT spectrum:<sup>27</sup>

$$f_c = \frac{1}{2}(f_1 + f_2), \quad (8)$$

$$\text{BW} = \frac{f_2 - f_1}{f_c} \times 100\%, \quad (9)$$

where  $f_1$  and  $f_2$  represent the lower and upper  $-6 \text{ dB}$  frequencies, respectively. The two-way insertion loss (IL) or the relative pulse-echo sensitivity is the ratio of the transducer output power  $P_o$  to the input power  $P_i$  delivered to the transducer from a driving source. If the output resistance  $R_o$  is assumed to be equal to the input resistance  $R_i$ , the two-way IL can be simplified as the ratio of the echo voltage  $V_o$  to the excitation voltage  $V_i$

$$\text{IL} = 10 \log \left( \frac{P_o}{P_i} \right) = 10 \log \left( \frac{V_o^2/R_o}{V_i^2/R_i} \right) = 20 \log \left( \frac{V_o}{V_i} \right). \quad (10)$$

The transducer was connected to a function generator (HP 8116A, USA) which was used to generate a tone burst of 20-cycle sine wave at  $f_c$ . The echo signal received by the transducer with  $V_o$  was measured by the oscilloscope with 1 M $\Omega$  coupling. The amplitude of the driving signal  $V_i$  was then measured with 50  $\Omega$  coupling. To investigate the temperature dependence of the transducer's performance, the transducer was heated with the silicone oil using an electrical heater. A thermometer was immersed into the silicone oil to record the temperature.

The waveforms and frequency spectra of the transducer measured at several temperatures were shown in Fig. 7. It can be seen that the echo response is still strong and clear with little ring-down even the temperature increases from room temperature to 165 °C. Figure 8 shows the calculated  $-6 \text{ dB}$  bandwidth and insertion loss of the transducer as a function of the temperature. It is shown that the bandwidth retains high values exceeding 100% from room temperature till 80 °C. The bandwidth decreases to 65% around 100 °C at which the rhombohedral-tetragonal phase transition of the single crystal takes place. The drop of the bandwidth is probably due to the variation of the resonant frequency at that temperature as shown in Fig. 4. Since the thickness of the matching layer was designed as one quarter wavelength of the active element frequency, the performance of the transducer would degrade if its resonant frequency shifts. Nevertheless, the echo signal is still sharp with little ring-down and reasonably high bandwidth. In the subsequent heating process, the bandwidth increases again. The phenomenon is very similar to that of the coupling coefficient  $k_t$  as shown in Fig. 4. It can be seen that transducer performance depends significantly on the characteristics of the transducer element. The transducer was found to exhibit 95% bandwidth at a high temperature of 165 °C. For the insertion loss, the variation is not big and the loss is generally getting better during the heating process. When the temperature exceeds 185 °C, no echo signal can be detected. It is because the transducer cannot work normally during the ferroelectric to paraelectric phase transition of the PIMNT single crystal near the Curie temperature.

#### IV. CONCLUSION

The PIMNT single crystal/epoxy 1–3 composites have been fabricated and investigated with various volume fractions of PIMNT single crystal. At room temperature, for the volume fractions ranging from 0.4 to 0.9,  $k_t$  remains at high value with a maximum value of 0.82. The experimental

parameters of the 1–3 composites agree quite well with the prediction of the modeling. Besides, it is shown that the composites can retain high electromechanical coefficient and stable acoustic properties within a wide temperature range from room temperature to 185 °C. With the superior performance, the composite with an optimal PIMNT volume fraction of 0.5 was used to fabricate a single-element ultrasonic transducer for high-temperature applications. It was found that the transducer exhibits a –6 dB bandwidth of 113% and the insertion loss of –32 dB at room temperature. When the temperature increases to 165 °C, it can still work normally with 95% bandwidth and –27 dB insertion loss. These results show that the PIMNT single crystal 1–3 composites have great potential for high-temperature ultrasonic applications.

## ACKNOWLEDGMENTS

This work was supported by the Hong Kong Innovative Technology Council (Project No. ITS/044/09FP).

- <sup>1</sup>R. F. Service, *Science* **275**, 1878 (1997).
- <sup>2</sup>S. E. Park and T. R. Shrout, *J. Appl. Phys.* **82**, 1804 (1997).
- <sup>3</sup>H. Luo, G. Xu, P. Wang, and Z. Yin, *Ferroelectrics* **231**, 97 (1999).
- <sup>4</sup>D. Damjanovic, M. Budimir, M. Davis, and N. Setter, *J. Mater. Sci.* **41**, 65 (2006).
- <sup>5</sup>L. Luo, H. Zhu, C. Zhao, H. Wang, and H. Luo, *Appl. Phys. Lett.* **90**, 52904 (2007).
- <sup>6</sup>D. Zhou, J. Chen, L. Luo, X. Zhao, and H. Luo, *Appl. Phys. Lett.* **93**, 073502 (2008).
- <sup>7</sup>S. T. Lau, K. H. Lam, H. L. W. Chan, C. L. Choy, H. Luo, Q. Yin, and Z. Yin, *Mater. Sci. Eng., B* **111**, 25 (2004).
- <sup>8</sup>Z. Feng, T. He, H. Xu, H. Luo, and Z. Yin, *Solid State Commun.* **130**, 557 (2004).
- <sup>9</sup>K. Harada, Y. Hosono, S. Saitoh, and Y. Yamashita, *Jpn. J. Appl. Phys.* **39**, 3117 (2000).
- <sup>10</sup>Y. Hosono, K. Harada, T. Kobayashi, K. Itsumi, M. Izumi, Y. Yamashita, and N. Ichinose, *Jpn. J. Appl. Phys.* **41**, 3808 (2002).
- <sup>11</sup>Y. Hosono, K. Harada, T. Kobayashi, K. Itsumi, M. Izumi, Y. Yamashita, and N. Ichinose, *Jpn. J. Appl. Phys.* **41**, 7084 (2002).
- <sup>12</sup>S. Zhang, J. Luo, W. Hackenberger, and T. R. Shrout, *J. Appl. Phys.* **104**, 064106 (2008).
- <sup>13</sup>Y. Guo, H. Luo, T. He, and Z. Yin, *Solid State Commun.* **123**, 417 (2002).
- <sup>14</sup>G. Xu, K. Chen, D. Yang, and J. Li, *Appl. Phys. Lett.* **90**, 032901 (2007).
- <sup>15</sup>J. Tian, P. Han, X. Huang, and H. Pan, *Appl. Phys. Lett.* **91**, 222903 (2007).
- <sup>16</sup>S. Zhang, J. Luo, W. Hackenberger, and T. R. Shrout, *J. Appl. Phys.* **104**, 064106 (2008).
- <sup>17</sup>H. P. Savakus, K. A. Klicker, and R. E. Newnham, *Mater. Res. Bull.* **16**, 677 (1981).
- <sup>18</sup>W. A. Smith and B. A. Auld, *IEEE Trans. Ultrason. Ferroelectr. Freq. Control* **38**, 40 (1991).
- <sup>19</sup>W. A. Smith, *IEEE Trans. Ultrason. Ferroelectr. Freq. Control* **40**, 41 (1993).
- <sup>20</sup>IEEE Standard on Piezoelectricity, ANSI/IEEE Std. 176 (1987).
- <sup>21</sup>G. S. Kino, *Acoustic Waves: Devices, Imaging, and Analog Signal Processing* (Prentice Hall, Englewood Cliffs, New York, 1987).
- <sup>22</sup>M. J. Zipparo, K. K. Shung, and T. R. Shrout, *IEEE Trans. Ultrason. Ferroelectr. Freq. Control* **44**, 1038 (1997).
- <sup>23</sup>See <http://www.smart-material.com/> for properties of moulded 1-3 composites.
- <sup>24</sup>H. Wang, H. Xu, T. He, X. Zhao, H. Luo, and Z. Yin, *Phys. Status Solidi A* **202**, 2829 (2005).
- <sup>25</sup>F. Wang, C. He, Y. Tang, X. Zhao, and H. Luo, *Mater. Chem. Phys.* **105**, 273 (2007).
- <sup>26</sup>C. S. Desilets, J. D. Fraser, and G. S. Kino, *IEEE Trans. Sonics Ultrason.* **SU-25**(3), 115 (1978).
- <sup>27</sup>American Institute of Ultrasound in Medicine (AIUM), “Standard methods for testing single-element pulse echo ultrasonic transducers,” *J. Ultrasound Med.* **1**, (1982).